CrystEngComm

COMMUNICATION

View Article Online
View Journal | View Issue



Cite this: *CrystEngComm*, 2016, **18**, 8999

Received 11th October 2016,
Accepted 3rd November 2016

DOI: 10.1039/c6ce02161a

www.rsc.org/crystengcomm



# Switchable oriented attachment and detachment of calcite nanocrystals†

Mihiro Takasaki, Yuya Oaki and Hiroaki Imai*

Switchable oriented attachment, *i.e.* reversible attachment and detachment, of nanocrystals was demonstrated in an aqueous system. Calcite nanoblocks unifaceted with {104} faces are reversibly attached and detached by swings of pH between 7 and 12.

In a classical model for crystal growth in solution systems, a crystalline body is enlarged through ion-by-ion addition routes. According to the well-known Ostwald ripening mechanism, large crystals grow by addition of ions supplied at the expense of smaller particles. In contrast, oriented attachment of small crystalline units was proposed as an alternative non-classical pathway for crystal growth in liquid media.[1–11] Crystal growth through oriented attachment was clearly observed in nanocrystal systems of chalcogenides,[12–14] metals,[15–17] and metal oxides.[18–21] In many previous reports, the oriented attachment of small building blocks was transiently observed during the growth process of relatively large crystalline architectures. Recently, we reported the formation of 1D alignment of calcite nanocrystals through controllable oriented attachment in an aqueous system at ambient temperatures.[22] The 1D alignment in the *c* direction can be ascribed to the partial Coulombic interaction of the calcite nanocrystals. The attachment is controllable by changing the basicity of the aqueous system and the collision frequency of the nanoblocks. However, the growth direction in oriented attachment has not been well controlled in previous studies. The reverse phenomenon, *i.e.* detachment of nanocrystals in the alignments that were formed through oriented attachment, has never been observed. In the present work, we show another type of reversible oriented attachment through large {104} faces of calcite nanoblocks by fine-tuning the pH of an aqueous system.

In various $CaCO_3$-based biominerals, mesoscopic granular textures that consist of oriented nanocrystals have been revealed with the incorporation of biological macromolecules.[23–27] Biogenic $CaCO_3$ crystals are composed of bridged nanograins or mesocrystals, in which isolated building blocks are arranged in the same crystallographic direction. Several formation routes to textured crystals and mesocrystals have been proposed that involve the oriented attachment of polymer-stabilized nanoparticles[28,29] and stepwise crystal growth with mineral bridges which connect nanoparticles.[30] Clarification of the oriented attachment routes for $CaCO_3$ is important for understanding biomineralization. Demineralization, including the dissolution of $CaCO_3$, is also essential for the morphogenesis of biominerals.[31] As a consequence, the detachment of $CaCO_3$ nanocrystals would be a notable biological phenomenon. If reversible oriented attachment and detachment of the building blocks are revealed, new findings could provide an important clue to elucidate biological mineralization and demineralization processes.

In the current work, we monitored the crystal growth through oriented attachment and dismantlement by the detachment of calcite nanocrystals with pH swings in their aqueous dispersion (Fig. 1). Although the unifaceted calcite nanocrystals were stably dispersed in the neutral pH region, we observed oriented attachment of the nanoblocks through {104} faces under a basic condition near the isoelectric point. Moreover, decreasing the pH induced the detachment of the

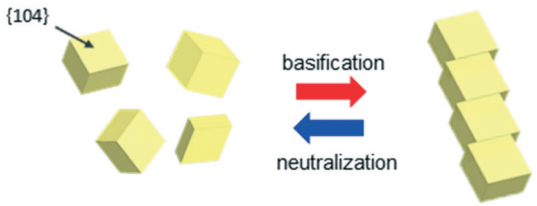


Fig. 1 Schematic illustration of the reversible, pH-sensitive oriented attachment of calcite rhombohedra covered with {104} faces.

*Department of Applied Chemistry, Faculty of Science and Technology, Keio University, 3-14-1 Hiyoshi, Kohoku-ku, Yokohama 223-8522, Japan.*
*E-mail: hiroaki@applc.keio.ac.jp*

† Electronic supplementary information (ESI) available. See DOI: 10.1039/c6ce02161a

nanoblocks from the alignments. To the best of our knowledge, this is the first report of the reversible, pH-sensitive oriented attachment and detachment of nanocrystals in an aqueous system.

Calcite nanoblocks were synthesized in a 200 $cm^3$ aqueous dispersion of 42.5 g $dm^{-3}$ $Ca(OH)_2$ through carbonation by introduction of $CO_2$ at a rate of 3.0 $dm^3$ $min^{-1}$. The pH of the dispersion (~13) started to decrease when the carbonation reaction was complete. The dispersion was then neutralized and adjusted to pH 7 by further introduction of $CO_2$ at 4 °C.

We monitored the change in the morphology of the calcite nanocrystals by the swing in the pH of the dispersion. After the neutral dispersion was maintained at 4 °C with stirring for a certain period (for example, 120 h), the dispersion of the calcite nanoblocks was then basified and adjusted to pH 12 by the addition of an alkaline solution (<5 $cm^3$) that was saturated with $Ca(OH)_2$. After being kept for another certain period (for example, 120 h), the alkaline dispersion of the calcite nanoblocks was neutralized and returned to pH 7 by the introduction of $CO_2$ and was maintained at 4 °C. We repeated these procedures to swing the pH of the dispersion.

The calcite nanoblocks (30–50 nm in diameter) were synthesized in a dispersion at pH 12 through the carbonation of $Ca(OH)_2$ in the aqueous system according to typical scanning electron microscopy (SEM) and X-ray diffraction (XRD) analysis (Fig. S1a and b†). Here, we show two kinds of oriented attachment of calcite nanoblocks. As reported in our previous work,[22] nanometric rods are elongated to ~1 μm long in the dispersion after stirring for several hundred hours at 4 °C (Fig. S1c†). The presence of the continuous lattice in the high-resolution transmission electron microscopy (HRTEM) image (Fig. S1d†) and fast Fourier transform (FFT) pattern (Fig. S1e†) confirmed that the calcite rods were a single crystal elongated in the *c* direction. On the other hand, the nanoblocks which are ~30–50 nm in size stably dispersed under a neutral condition for more than 120 h after carbonation (Fig. 2). In the TEM image, the single-crystalline grains were found to be roughly covered with {104} facets in the neutral dispersion. As compared with the grains in the basic dispersion, the {104} facets became clear when kept under a neutral condition.

As shown in Fig. 3, we observed another type of oriented attachment of isolated calcite nanocrystals through the {104} faces by the basification of their neutral dispersion with the addition of an alkaline solution that was saturated with $Ca(OH)_2$. After maintaining the dispersion at pH 12 for 120 h, winding and branching chains were formed by connecting the nanoblocks. The outlines of the nanoblocks in the chains are parallel to each other and can be assigned to the edges of a calcite rhombohedron that is covered with {104} faces. This feature is clearly different from the 1D chains of the calcite nanoblocks elongated in the *c* direction (Fig. S1c†). The HRTEM images and their FFT patterns indicate that the nanocrystals were covered with {104} faces (Fig. 4a and S2a†). Moreover, the faceted nanoblocks were found to be attached to each other by the {104} faces (Fig. 4b and S2b†). We observed that most of the rhombohedra (more than 95%) formed chains through the oriented attachment in the dispersion.

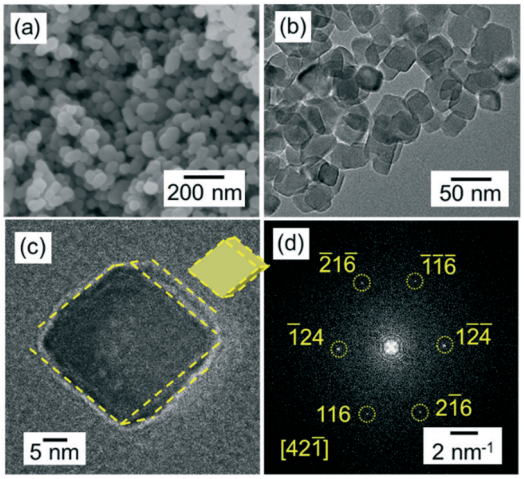


**Fig. 2** SEM (a), TEM (b), and HRTEM (c) images of the calcite nanoblocks that were dispersed stably under a neutral condition (pH 7) for more than 120 h after carbonation; the FFT pattern (d) of the calcite nanoblocks in (c). The grains in (a) and (b) were randomly aggregated during the drying process. (c) Yellow dashed lines indicate the edges of the {104} faces of a calcite rhombohedron.

The basic dispersion of the nanochains was neutralized and returned to pH 7 by the renewed introduction of $CO_2$. As shown in Fig. 5, the chains disappeared, and the isolated nanoblocks exhibiting {104} facets were observed in the resultant neutral dispersion. The size distribution of the isolated nanoblocks in the resultant dispersion was almost the same as that of the grains in the initial dispersion (Fig. S3†). These results indicate that the calcite nanocrystals were reproduced by the disjuncture of the chains. The similarity of sizes and shapes of the initial and resultant blocks, suggests that the original calcite nanocrystals are detached by neutralization.

The pH-sensitive attachment and detachment of the calcite nanocrystals have been found to be reversible. We elevated the pH of the dispersion again by the renewed addition of calcium solution saturated with $Ca(OH)_2$. As shown in Fig. 6, the chains consisting of the nanoblocks were formed again by basification. The outlines of the nanoblocks in the chains are parallel to each other and can be assigned to the edges of

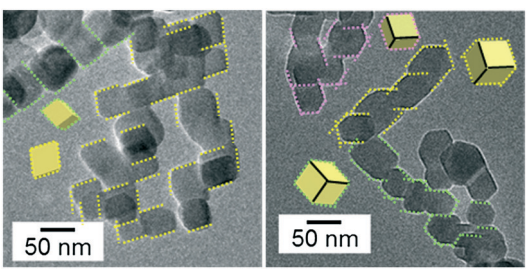


**Fig. 3** TEM images of the chains consisting of calcite nanoblocks in a basic dispersion (pH 12) kept for 120 h. Yellow, green, and pink dashed lines indicate the edges of the {104} faces of a calcite rhombohedron. Each color indicates rhombohedra having the same orientation.

 

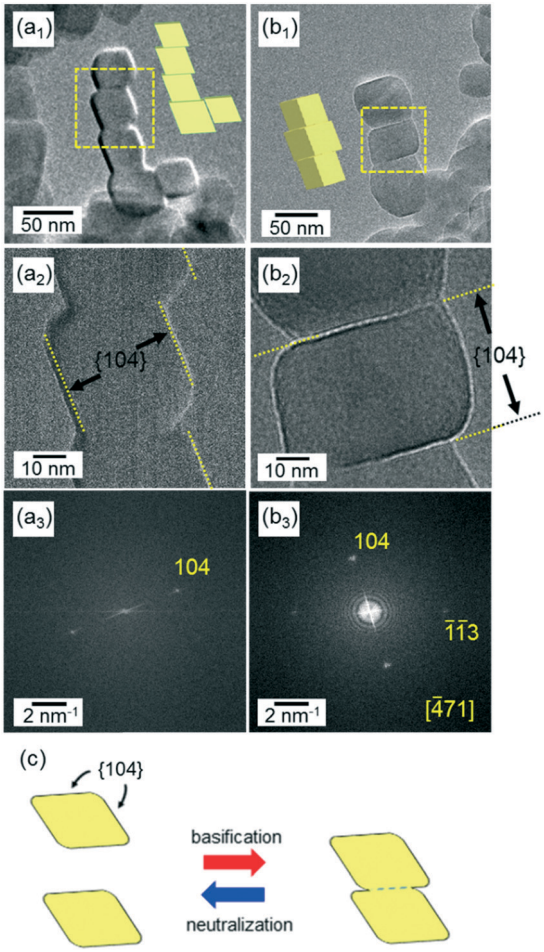


Fig. 4 HRTEM images ($a_{1\ and\ 2}$ and $b_{1\ and\ 2}$) and the FFT patterns ($a_3$ and $b_3$) of adjacent calcite nanoblocks in the chains of the basic dispersion (pH 12) kept for 120 h. The FFT pattern ($a_3$) indicates that the nanoblocks are covered with {104} faces. In this case, the nanoblocks are suggested to be attached through the {104} faces, as shown in ($a_1$). The FFT pattern ($b_3$) indicates that the nanoblocks are attached through the {104} faces, as shown in ($b_1$). The fringes of the calcite lattices can be observed on the enlarged HRTEM images (Fig. S2†). Schematic illustration (c) of the attachment and detachment of the two unifaceted rhombohedra through the {104} faces under a basic condition and a neutral condition, respectively.

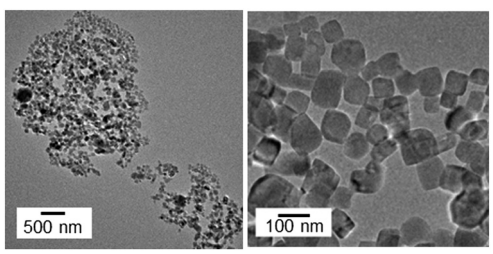


Fig. 5 TEM images of the nanoblocks by the disjuncture of the chains in a dispersion maintained at pH 7 for 24 h after neutralization.

a calcite rhombohedron that is covered with {104} faces. Thus, the basification induced the attachment of calcite nanoblocks in the dispersion by the {104} faces. When the basic dispersion of the nanochains was returned to pH 7 by

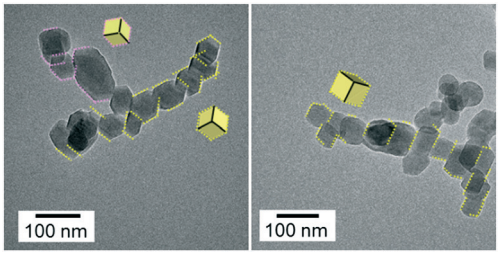


Fig. 6 TEM images of the chains of the calcite nanoblocks that reproduced in a dispersion maintained at pH 12 for 24 h. Yellow and pink dotted lines indicate the edges of {104} faces. Each color indicates rhombohedra having the same orientation. Several large grains would be formed by Ostwald ripening during swings of pH.

the renewed introduction of $CO_2$, the chains disappeared, and the isolated nanoblocks that exhibited {104} facets were then observed in the resultant neutral dispersion. The repeatability indicates that the oriented attachment and detachment are reversible by swings of pH.

Fig. 1 shows a schematic illustration of the reversible, pH-sensitive oriented attachment and detachment of calcite nanoblocks. In an aqueous medium, faceted calcite nanoblocks are attached under a basic condition and detached under a neutral condition. Calcite nanoblocks are stably dispersed because their surface is positively charged outside the isoelectric point (pH 11.5). Because the surface charge is negligible in an aqueous dispersion at a pH around the isoelectric point, blocks are easily attached to each other without a repulsion force. In the case of the nanograins that exhibit defined {104} facets, oriented attachment occurs through the large stable faces. When the facet formation is insufficient, the calcite nanoblocks attach in the *c* direction due to their dipole moment that originates from the Coulombic interaction of the *c* faces as reported in our previous work.[22] In the present study, we have shown the former type of the alignment under a basic condition.

Calcites are generally known to form rhombohedral grains unifaceted with {104} faces due to their high stability.[32,33] The {104} face is the most stable facet of calcites due to its neutrality and flat ion arrangement (Fig. S4†). Thus, rhombohedral calcite grains are gradually formed in a neutral aqueous system. In the TEM images (Fig. 2), we confirmed the formation of the rhombohedra from the lattice fringes and their shapes. The solubility of calcite in an aqueous system is $2.5 \times 10^{-6}$ mol dm$^{-3}$ at pH 12 and $3.2 \times 10^{-3}$ mol dm$^{-3}$ at pH 7.[34] The solid concentration of calcite grains in our system was $5.6 \times 10^{-1}$ mol dm$^{-3}$. An increase in the ion concentration with pH variation is compensated by partial dissolution (<1%) of the solid grains. Thus, the size reduction is negligible due to partial dissolution of the nanoblocks when the pH is decreased to 7. Therefore, the nanoblocks are attached through the enlarged {104} faces by elevating the basicity of the dispersion after being kept under a neutral condition for a certain period.

The detachment of the nanoblocks occurs by neutralization. As the pH of the dispersion decreases to around 7,

calcite is partially dissolved as the solubility increases. As shown in Fig. 4b$_2$, the {104} planes and the necking parts were clearly observed at the boundaries between the original rhombohedra. The attached interface would be dissolved easily due to the presence of defects, dislocations, and necking parts (Fig. 4b$_2$ and c). Thus, the nanoblocks in the chains are detached and returned to grains of the original size. The detached particles are stably dispersed due to their positive surface charge. The pH-sensitive oriented attachment and detachment of calcite rhombohedra can be reversed by changing the pH of the aqueous system.

The attachment through the {104} faces occurs easily because the surfaces are not charged. Moreover, the lattices match each other due to the flatness of the ion configuration. On the other hand, some defects remain at the boundary formed by the attachment of two {104} planes. Thus, detachment of the grains occurs because the boundary is easily attached even under a neutral condition.

In summary, we monitored the reversible attachment and detachment of calcite nanocrystals by pH swings in an aqueous system. The nanoblocks are stably dispersed due to their surface charges. Attachment is induced through the {104} facets by the disappearance of the surface charge under a basic condition near the isoelectric point. Detachment occurs through partial dissolution at the boundary between the binding grains as the solubility is increased by decreasing the pH. The detached nanograins have a high dispersivity due to their surface charge. Finally, swings of the pH lead to the reversible attachment and detachment of the nanoblocks. Our findings on the reversible, pH-sensitive oriented attachment of calcite, which is a main component of biominerals, would be helpful for understanding the biogenic and biomimetic mineralization and demineralization processes.

## Acknowledgements

This work was partially supported by the Kato Foundation for Promotion of Science, a Grant-in-Aid for Challenging Exploratory Research (15K14129), and a Grant-in-Aid for Scientific Research (A) (16H02398) from Japan Society for the Promotion of Science.

## References

1 H. Cölfen and S. Mann, *Angew. Chem., Int. Ed.*, 2003, **42**, 2350.
2 J. J. De Yoreo, P. U. Gilbert, N. A. Sommerdijk, R. L. Penn, S. Whitelam, D. Joester, H. Zhang, J. D. Rimer, A. Navrotsky, J. F. Banfield, A. F. Wallace, F. M. Michel, F. C. Meldrum, H. Cölfen and P. M. Dove, *Science*, 2015, **349**, 498.
3 R. L. Penn and J. F. Banfield, *Geochim. Cosmochim. Acta*, 1999, **63**, 1549.
4 J. F. Banfield, S. A. Welch, H. Zhang, T. T. Ebert and R. L. Penn, *Science*, 2000, **289**, 751.
5 C. Pacholski, A. Kornowski and H. Weller, *Angew. Chem.*, 2002, **114**, 1234.
6 M. Niederberger and H. Cölfen, *Phys. Chem. Chem. Phys.*, 2006, **8**, 3271.
7 A. E. S. Van Driessche, L. G. Benning, J. D. Rodriguez-Blanco, M. Ossorio, P. Bots and J. M. García-Ruiz, *Science*, 2012, **336**, 69.
8 T. M. Stawski, A. E. S. van Driessche, M. Ossorio, J. D. Rodriguez-Blanco, R. Besselink and L. G. Benning, *Nat. Commun.*, 2016, **7**, 11177, DOI: 10.1038/ncomms11177.
9 W. He, *CrystEngComm*, 2014, **16**, 1439.
10 Y. Zhang, W. He, K. Wen, X. Wang, H. Lu, X. Lin and J. H. Dickerson, *Analyst*, 2014, **139**, 371.
11 W. Lv, W. He, X. Wang, Y. Niu, H. Cao, J. H. Dickerson and Z. Wang, *Nanoscale*, 2014, **6**, 2531.
12 W. Koh, A. C. Bartnik, F. W. Wise and C. B. Murray, *J. Am. Chem. Soc.*, 2010, **132**, 3909.
13 Z. Tang, N. A. Kotov and M. Giersig, *Science*, 2002, **297**, 237.
14 K. S. Cho, D. V. Talapin, W. Gaschler and C. B. Murray, *J. Am. Chem. Soc.*, 2005, **127**, 7140.
15 A. Halder and N. Ravishankar, *Adv. Mater.*, 2007, **19**, 1854.
16 Y. Wang, S. Choi, X. Zhao, S. Xie, H. C. Peng, M. Chi and Y. Xia, *Adv. Funct. Mater.*, 2014, **24**, 131.
17 H. Ataee-Esfahani and S. E. Skrabalak, *RSC Adv.*, 2015, **5**, 47718.
18 C. Pacholski, A. Kornowski and H. Weller, *Angew. Chem., Int. Ed.*, 2002, **41**, 1188.
19 N. Du, H. Zhang, B. Chen, X. Ma and D. Yang, *J. Phys. Chem. C*, 2007, **111**, 12677.
20 Y. Nakagawa, H. Kageyama, R. Matsumoto, Y. Oaki and H. Imai, *CrystEngComm*, 2015, **17**, 7477.
21 A. Chen, Y. Zhou, S. Miao, Y. Li and W. Shen, *CrystEngComm*, 2016, **18**, 580.
22 M. Takasaki, Y. Oaki and H. Imai, *RSC Adv.*, 2016, **6**, 61346.
23 Y. Oaki, A. Kotachi, T. Miura and H. Imai, *Adv. Funct. Mater.*, 2006, **16**, 1633.
24 M. Kijima, Y. Oaki and H. Imai, *Chem. – Eur. J.*, 2011, **17**, 2828.
25 A. Hayashi, T. Watanabe and T. Nakamura, *Zoology*, 2010, **113**, 125.
26 M. Suzuki, T. Kogure, S. Weiner and L. Addadi, *Cryst. Growth Des.*, 2011, **11**, 4850.
27 S. Mann, *J. Chem. Soc., Dalton Trans.*, 1993, 1.
28 F. Dang, K. Kato, H. Imai, S. Wada, H. Haneda and M. Kuwabara, *Cryst. Growth Des.*, 2011, **11**, 4129.
29 K. X. Yao, X. M. Yin, T. H. Wang and H. C. Zeng, *J. Am. Chem. Soc.*, 2010, **132**, 6131.
30 Y. Oaki, S. Hayashi and H. Imai, *Chem. Commun.*, 2007, 2841.
31 A. Ziegler, D. Weihrauch, M. Hagedorn, D. W. Towle and R. Bleher, *J. Exp. Biol.*, 2004, **207**, 1749.
32 D. Aquilano, E. Costa, A. Genovese, F. R. Massaro, L. Pastero and M. Rubbo, *J. Cryst. Growth*, 2003, **247**, 516.
33 B. R. Heywood, S. Dajam and S. Mann, *J. Chem. Soc., Faraday Trans.*, 1991, **87**, 735.
34 W. Stumm and J. J. Morgan, *Aquatic chemistry: chemical equilibria and rates in natural waters*, John Wiley & Sons, 3rd edn, 2012, p. 374.

 